

Experiment, theory and the Casimir effect

V. M. Mostepanenko¹

Center of Theoretical Studies and Institute for Theoretical Physics, Leipzig University,
Vor dem Hospitaltore 1, 100920, D-04009, Leipzig, Germany

E-mail: vladimir.mostepanenko@itp.uni-leipzig.de

Abstract. Several problems at the interface between the field-theoretical description of the Casimir effect and experiments on measuring the Casimir force are discussed. One of these problems is connected with the definition of the Casimir free energy in ideal metal rectangular boxes satisfying the general physical requirements. It is shown that the consideration of rectangular boxes with a partition (piston) does not negate the previously known results obtained for boxes without a piston. Both sets of results are found to be in mutual agreement. Another problem is related to the use of the proximity force approximation for the interpretation of the experimental data and to the search of analytical results beyond the PFA based on the first principles of quantum field theory. Next, we discuss concepts of experimental precision and of the measure of agreement between experiment and theory. The fundamental difference between these two concepts is clarified. Finally, recent approach to the thermal Casimir force taking screening effects into account is applied to real metals. It is shown that this approach is thermodynamically and experimentally inconsistent. The physical reasons of this inconsistency are connected with the violation of thermal equilibrium which is the basic applicability condition of the Lifshitz theory.

1. Introduction

For almost 50 years since Casimir's discovery [1], theory existed independent of rare experiments [2,3]. A lot of theoretical work has been done during this period. However, the relationship to reality of some theoretical models, such as an ideal metal spherical shell, an ideal metal rectangular box, a dielectric ball etc., remains unclear up to now. In the last ten years scientific investigations in the field of the Casimir effect have experienced an interaction between experiment and theory. This has revealed that the application of some basic theories to real experimental situations is highly nontrivial and even leads to communication difficulties between theorists and experimentallists.

In this paper we summarize some experience of the interaction between "high theory" and real world experimental details in the last ten years. Different points of view are considered on such problems as agreement between experiment and theory and applicability of some ideal models and approximate methods in real experimental situations. It is shown that in some cases confusion arises from an inadequate use of terminology.

In Sec. 2 we discuss an old problem of the thermal Casimir force in ideal metal rectangular boxes and suggest a new solution which satisfies general physical criteria. It is shown that the case of an isolated box is independent of a box with a partition (piston). The results for the Casimir force obtained for each of these configurations are in mutual agreement.

¹ On leave from Noncommercial Partnership "Scientific Instruments", Moscow, Russia

Section 3 briefly reviews the proximity force approximation including its justification from the first principles of quantum field theory and experimental applications. In this respect a new representation for the Casimir energy in terms of the functional determinants and scattering matrices is considered. The application of this representation to real material bodies is still problematic.

In Sec. 4 we consider the problem of the reliability of experiments. It is underlined that the experimental error is an independent characteristic of the experimental precision which should not be confused with the measure of agreement between experiment and theory.

Section 5 is devoted to the comparison between experiment and theory in the measurements of the Casimir force. In this respect different approaches to the theoretical description of the Casimir force between real metals are compared with the most precise indirect measurement of the Casimir pressure between two parallel plates by means of micromechanical torsional oscillator [4,5]. Special attention is paid to uncertainties which might be introduced in the computations due to deviations of the tabulated optical data from the data particular to the metallic films actually used.

In Sec. 6 we consider a recent theoretical approach to the thermal Casimir force taking into account the screening effects and diffusion currents. We apply this approach to the case of real metals and analyze its consistency with the principles of thermodynamics and experimental data. Specifically we show that for metals with perfect crystal lattices the inclusion of screening effects results in violation of the Nernst heat theorem. The experimental data of the experiment [4,5] exclude this approach at a 99.9% confidence level.

Section 7 contains our conclusions and discussion.

2. Thermal Casimir force in ideal metal rectangular boxes

Ideal metal rectangular boxes were first considered by Lukosz [6], Mamayev and Trunov [7,8] and Ambjørn and Wolfram [9]. This configuration attracted much attention because it was found that the electromagnetic Casimir force in rectangular boxes can be both attractive and repulsive depending on the ratio of sides a_x , a_y and a_z along the x , y and z axes. The nonrenormalized Casimir energy of the box is equal to (for simplicity we consider the massless scalar field with Dirichlet boundary conditions)

$$E_0(a_x, a_y, a_z) = \frac{\hbar}{2} \sum_{n,l,p=1}^{\infty} \omega_{nlp}, \quad (1)$$

where

$$\omega_{nlp} = \pi c \left[\left(\frac{n}{a_x} \right)^2 + \left(\frac{l}{a_y} \right)^2 + \left(\frac{p}{a_z} \right)^2 \right]^{1/2}. \quad (2)$$

The regularization of (1) can be performed, e.g., using the Epstein zeta function or the cut-off method [10]. The latter permits to find the geometric structure of infinities contained in (1). To do so, one replaces $E_0(a_x, a_y, a_z)$ from (1) with $E_0^{(\delta)}(a_x, a_y, a_z)$ by introducing the cut-off function

$$f(\delta\omega_{nlp}) = e^{-\delta\omega_{nlp}} \quad (3)$$

under the sign of summation in (1). After the repeated application of the Abel-Plana formula [10] to $E_0^{(\delta)}(a_x, a_y, a_z)$ one finds that there are three different types of divergent quantities in the limit $\delta \rightarrow 0$, I_1 , I_2 and I_3 of order δ^{-4} , δ^{-3} and δ^{-2} , respectively. Then, the finite, renormalized, Casimir energy can be defined as

$$E_0^{\text{ren}}(a_x, a_y, a_z) = \lim_{\delta \rightarrow 0} \left[E_0^{(\delta)}(a_x, a_y, a_z) - I_1 - I_2 - I_3 \right]. \quad (4)$$

Here, I_k ($k = 1, 2, 3$) are the counter terms having the following geometrical structure:

$$I_1 = \frac{12\pi^2\hbar a_x a_y a_z}{c^3\delta^4}, \quad I_2 = -\frac{\pi^2\hbar(a_x a_y + a_x a_z + a_y a_z)}{c^2\delta^3}, \quad I_3 = \frac{\pi\hbar(a_x + a_y + a_z)}{8c\delta^2}. \quad (5)$$

A similar situation takes place for the electromagnetic field, where the renormalized Casimir energy, $E_{0,\text{em}}^{\text{ren}}$, also takes the form of (4) (with E_0 replaced for E_0^{em}) and

$$I_1^{\text{em}} = 2I_1, \quad I_2^{\text{em}} = 0, \quad I_3^{\text{em}} = -2I_3. \quad (6)$$

It is seen that in both cases the counter terms are proportional to the volume of the box $V = a_x a_y a_z$, to the area of box surface and to the sum of sides.

In the last few years the configuration of a rectangular box with so-called *movable* partition (piston) has attracted much attention [11–14]. This means that the piston can have any fixed position parallel to the two opposite faces of the box (the configuration where the piston is not fixed and may slide between the opposite faces is in fact a nonequilibrium case). Let the piston be parallel to the plane xy and have an equation $z = a_{z1} < a_z$. In this case our box is divided into the two boxes $a_x \times a_y \times a_{z1}$ and $a_x \times a_y \times (a_z - a_{z1})$. Calculating the sum of the regularized Casimir energies

$$E_0^{(\delta)}(a_x, a_y, a_{z1}) + E_0^{(\delta)}(a_x, a_y, a_z - a_{z1}), \quad (7)$$

one finds that the contribution from the singular terms of the form of (5) does not depend on the position of the piston a_{z1} . This leads to a finite force acting on the piston

$$F(a_x, a_y, a_z, a_{z1}) = -\frac{\partial}{\partial a_{z1}} \left[E_0^{(\delta)}(a_x, a_y, a_{z1}) + E_0^{(\delta)}(a_x, a_y, a_z - a_{z1}) \right]. \quad (8)$$

This force is well defined and does not require the renormalization procedure (4).

In both scalar and electromagnetic cases the force acting on the piston attracts it to the nearest face of the box. On this ground the existence of the Casimir repulsion in cubes in the electromagnetic case was considered doubtful [12]. Specifically, it was claimed [12,13] that the definition of the pressure acting on a cube face requires elastic deformations of single bodies treated as perfect. The attraction (or repulsion for a piston with Neumann boundary conditions [15]) of a piston to the nearest face of the box does not, however, negate the Casimir repulsion for boxes without a piston that have some appropriate ratio of a_x , a_y and a_z . The point is that the cases with an empty space outside the box and that with another section of the larger box outside the piston are physically quite different. In the first case the vacuum energy outside the box does not depend on a_x , a_y and a_z and there is no force acting on the box from the outside. Whereas in the second case there is an extra section of the larger box outside the piston which gives rise to the additional force acting on it. In fact one need not admit elastic deformations to define a force and a pressure in static configurations. This is simply done using the principle of virtual work and virtual displacements through real forces [16,17]. In addition, from a thermodynamic point of view any equilibrium system can be characterized by the free energy (energy if the temperature is equal to zero) and the respective pressure [18]

$$P = -\left. \frac{\partial \mathcal{F}}{\partial V} \right|_{T=\text{const}}. \quad (9)$$

From this point of view it would be illogical to admit consideration of the force acting on a piston, but exclude from consideration forces acting on the faces of a box where this piston serves as a partition.

In this respect it seems important to provide a finite definition of the Casimir free energy in ideal metal rectangular boxes satisfying general physical requirements. The first calculations

on this subject [9] resulted in a divergent free energy after removing the regularization. More recent results appear to be either infinite [19] or ambiguous [20]. Paper [21] reconsidered the derivation of the Casimir free energy in rectangular boxes using zeta functional regularization. However, the used formalism does not include all necessary subtractions.

The following definition of the Casimir free energy in rectangular boxes suggests itself [12,13,21]

$$\mathcal{F}_0 = E_0^{\text{ren}} + \Delta_T \mathcal{F}_0, \quad \Delta_T \mathcal{F}_0 = k_B T \sum_{n,l,p=1}^{\infty} \ln \left(1 - e^{-\frac{\hbar \omega_{nlp}}{k_B T}} \right). \quad (10)$$

This expression is finite. However, it cannot be considered as physically satisfactory. The problem is that at high temperature the thermal correction (10) behaves as [22]

$$\Delta_T \mathcal{F}_0 = \alpha_1 \frac{(k_B T)^4}{(\hbar c)^3} + \alpha_2 \frac{(k_B T)^2}{(\hbar c)^2} + \alpha_3 \frac{(k_B T)^2}{\hbar c} + \alpha_4 k_B T + \dots, \quad (11)$$

where $\alpha_1 = -V\pi^2/90$, $\alpha_{2,3} = \alpha_{2,3}(a_x, a_y, a_z)$ can be expressed in terms of the heat kernel coefficients and $\alpha_4 = \text{const}$. Then at high temperature $\Delta_T \mathcal{F}_0$ contains terms of quantum origin which increase with the increase of temperature. In the general case, these terms lead to respective forces acting on the box faces which increase with the increase of the sides of the box. Such paradoxical properties are physically unacceptable. Because of this it was suggested [23] to define the physical Casimir free energy of the box as

$$\mathcal{F} = E_0^{\text{ren}} + \Delta_T \mathcal{F}_0 - \alpha_1 \frac{(k_B T)^4}{(\hbar c)^3} - \alpha_2 \frac{(k_B T)^2}{(\hbar c)^2} - \alpha_3 \frac{(k_B T)^2}{\hbar c}. \quad (12)$$

With this definition, the respective Casimir forces acting on the box faces go to zero when all the box sides a_x , a_y , a_z go to infinity in agreement with physical intuition.

The physical meaning of all three subtractions made on the right-hand side of (12) can be clearly understood. The first term is actually the contribution of the blackbody radiation in the volume of the box. This is seen from the fact that the free energy density of the blackbody radiation in empty space is given by

$$f_{bb} = k_B T \int \frac{d^3 k}{(2\pi)^3} \ln \left(1 - e^{-\frac{\hbar c |k|}{k_B T}} \right) = -\frac{\pi^2 (k_B T)^4}{90 (\hbar c)^3}, \quad (13)$$

where for the electromagnetic case $f_{bb}^{\text{em}} = 2f_{bb}$.

For the scalar Casimir effect in a rectangular box with sides $a_x \times a_y \times a_z$ the asymptotic behavior of $\Delta_T \mathcal{F}_0$ at high T was investigated in [23] with the result

$$\alpha_2 = \frac{\zeta(3)}{4\pi} (a_x a_y + a_x a_z + a_y a_z), \quad \alpha_3 = -\frac{\pi}{24} (a_x + a_y + a_z). \quad (14)$$

In the electromagnetic case the following values of these coefficients were obtained:

$$\alpha_2^{\text{em}} = 0, \quad \alpha_3^{\text{em}} = \frac{\pi}{12} (a_x + a_y + a_z). \quad (15)$$

This demonstrates that the geometric structures of all three terms subtracted in (12) are precisely the same as the terms subtracted in (4) to make the Casimir energy finite at zero temperature. Because of this, the subtraction procedure in (12) can be interpreted as the additional (finite) renormalization of the same geometric parameters as were renormalized at zero temperature to make the Casimir energy of the box finite.

The simplest application of the final expression for the physical Casimir free energy (12) is the case of two plane parallel plates. It is easily seen that in this configuration $\alpha_2 = \alpha_3 = 0$ and one is left with only a subtraction of the free energy of the blackbody radiation in the volume between the plates $V = aS$, where S is the infinite plate area. This leads to the well known result [10,24] for the electromagnetic Casimir free energy per unit area of the plates

$$\mathcal{F}(a, T) = -\frac{\pi^2}{720a^3} \left\{ 1 + \frac{45}{\pi^3} \sum_{l=1}^{\infty} \left[\frac{\coth(\pi lt)}{t^3 l^3} + \frac{\pi}{t^2 l^2 \sinh^2(\pi tl)} \right] - \frac{1}{t^4} \right\}, \quad (16)$$

where $t \equiv T_{\text{eff}}/T$, and the effective temperature is defined as $k_B T_{\text{eff}} = \hbar c/(2a)$. In particular, at $T \ll T_{\text{eff}}$ one obtains

$$\mathcal{F}(a, T) = -\frac{\pi^2}{720a^3} \left[1 + \frac{45\zeta(3)}{\pi^3} \left(\frac{T}{T_{\text{eff}}} \right)^3 - \left(\frac{T}{T_{\text{eff}}} \right)^4 \right], \quad (17)$$

where the last contribution on the right-hand side originates from the subtraction of the blackbody radiation. We emphasize that only this term contributes to the thermal correction to the electromagnetic Casimir pressure at low temperatures (short separations)

$$P(a, T) = -\frac{\pi^2}{240a^4} \left[1 + \frac{1}{3} \left(\frac{T}{T_{\text{eff}}} \right)^4 \right]. \quad (18)$$

Equation (12) solves the long-standing problem on the calculation of the physical Casimir free energies and pressures in rectangular boxes of any size. A few examples for both the scalar and electromagnetic Casimir effect are considered in [23]. Here we present the computational results for the electromagnetic free energy in a cube and for the respective Casimir force

$$F_x(a, T) = a^2 P(a, T) = -\frac{1}{3} \frac{\partial \mathcal{F}(a, T)}{\partial a} \quad (19)$$

acting on the opposite cube faces.

In Fig. 1(a) we plot the electromagnetic Casimir free energy in a cube as a function of a at $T = 300$ K (solid line). In the same figure the Casimir energy at $T = 0$ is shown by the dashed line. As is seen in this figure, the electromagnetic Casimir free energy decreases with the increase of separation. At large separations \mathcal{F} approaches a constant. In Fig. 1(b) the electromagnetic Casimir free energy is shown as a function of temperature for a cube with $a = 2 \mu\text{m}$. The free

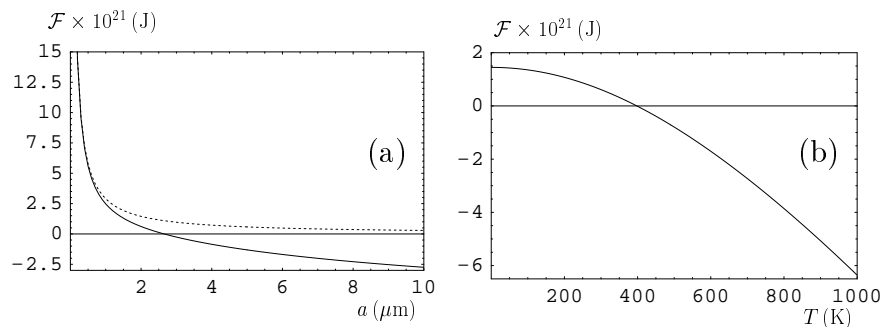


Figure 1. The electromagnetic Casimir free energy for a cube as a function of (a) size a at $T = 300$ K (solid line; the dashed line shows the energy at $T = 0$) and (b) temperature at $a = 2 \mu\text{m}$.

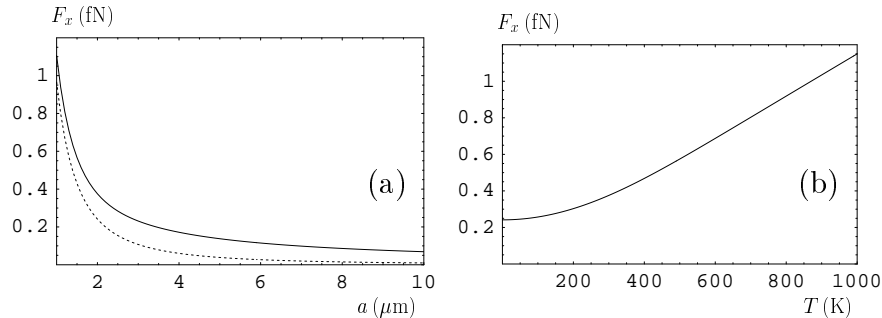


Figure 2. The electromagnetic Casimir force between the opposite faces of a cube as a function of (a) size a at $T = 300\text{ K}$ (solid line; the dashed line shows the force at $T = 0$) and (b) temperature at $a = 2\ \mu\text{m}$.

energy decreases with the increase of T . At high temperatures \mathcal{F} demonstrates the classical limit. The respective thermal electromagnetic Casimir force at $T = 300\text{ K}$, as a function of a , is shown in Fig. 2(a) by the solid line. It is positive (i.e., repulsive) for cubes of any size. Thus, thermal effects for cubes in the electromagnetic case increase the strength of the Casimir repulsion. The dashed line in Fig. 2(a) shows the electromagnetic Casimir force at $T = 0$ as a function of a . This force is given by

$$F_x(a) = \frac{0.09166}{3a^2}, \quad (20)$$

i.e., it is always repulsive. Fig. 2(b) demonstrates the electromagnetic Casimir force in a cube of size $a = 2\ \mu\text{m}$ as a function of temperature. It is seen that the force increases with increasing temperature.

Note that the results presented differ from those found in [21] where the terms of order $(k_B T)^4$ and of lower orders in the Casimir free energy were obtained in the high-temperature regime. This is explained by the fact that the authors of [21] did not make subtractions of the contributions from the blackbody radiation and of the terms proportional to the box surface area and to the sum of its sides.

The thermal correction to the Casimir energy and force acting on a piston were investigated in [13] for the scalar field with Dirichlet or Neumann boundary conditions using the definition (10). The electromagnetic Casimir free energy and force acting on a piston were found in the case of ideal metal rectangular boxes and cavities with the general cross section [13]. In the limit of low temperatures the thermal correction to the Casimir force on a piston was shown to be exponentially small. In the case of medium temperature $a_x \ll \hbar c / (k_B T) \ll a_y, a_z$ the authors of [13] obtained terms of order $(k_B T)^4$ and of order $(k_B T)^2$ in the electromagnetic Casimir free energy. In the scalar Casimir free energy, a term of order $(k_B T)^3$ was also obtained. This results in the contribution to the force acting on a piston which increases with the increase of the temperature, depends on \hbar and c and does not depend on the position of the piston. The scalar and electromagnetic thermal Casimir forces acting on a piston were also considered on the basis of equation (10) in [25].

The same results for the thermal correction to the Casimir force acting on a piston are obtained if the free energy is defined in accordance with equation (12). This is because the contribution of blackbody radiation to the energy of the entire box is equal to

$$-a_x a_y a_{z1} f_{bb} - a_x a_y (a_z - a_{z1}) f_{bb} = -a_x a_y a_z f_{bb}, \quad (21)$$

i.e., it does not depend on the position of the piston. This is also true for terms of order $(k_B T)^3$

and $(k_B T)^2$ which are proportional to the surface area of each section of the box and to the sum of its sides.

The above results were obtained for rectangular boxes with the Dirichlet boundary conditions (scalar case) and for ideal metal boxes (electromagnetic case). In the same way, as for zero temperature, the consideration of the thermal Casimir effect in rectangular boxes has to incorporate real material properties of the boundary surfaces. Till now this problem has not been conclusively solved.

3. Functional determinants and the justification of the proximity force approximation

The proximity force approximation [26] provides an important bridge between experiment and theory. Experimentally it is hard to use the configuration of two parallel plates. Because of this, most of experiments use the configuration of a sphere above a plate for which, even in the ideal metal case, the exact results for the electromagnetic Casimir force are not available. According to the proximity force approximation (PFA), the interaction energy between two curved surfaces Σ_1 and Σ_2 can be approximately calculated by replacing the small curved surface elements with respective plane plates. If the interaction energy between the opposite plane parallel elements is notated as $E(z)$ (where z is the separation distance), the interaction energy and force are approximately represented as

$$U(a) = \int_{\Sigma_1} E(z) d\sigma, \quad F(a) = -\frac{\partial U(a)}{\partial a}. \quad (22)$$

For the configuration of an ideal metal sphere of radius R at a separation a above an ideal metal plane (22) results in

$$F_{\text{PFA}}^s(a) = 2\pi R E(a) = -\frac{\pi^3 \hbar c R}{360 a^3}. \quad (23)$$

For an ideal metal cylinder above an ideal metal plate the PFA leads to

$$F_{\text{PFA}}^c(a) = \frac{15\pi}{16} \sqrt{\frac{2R}{a}} E(a) = -\frac{\pi^3}{384\sqrt{2}} \sqrt{\frac{R}{a}} \frac{\hbar c}{a^3}. \quad (24)$$

Equations (22)–(24) are the approximate ones. They are applicable only at short separations between the surfaces. Thus, (23) and (24) work well only at $a \ll R$.

In many papers the PFA (22) is applied in a region where it is not applicable, for example at $a = R/2$. The obtained large deviations of the PFA result from the exact result are then considered as a “violation of the PFA”. Such formulations are in fact misleading. The PFA gives only the main contribution to the force under some conditions. Specifically, it would be meaningless to calculate the integral in (22) up to higher orders in the related small parameter with the aim of obtaining a more exact result. What is really meaningful is the search of an exact analytical representation for the Casimir force in configurations where only the PFA result is so far available.

In the last few years the finite representation for the Casimir energy for two separated bodies A and B in terms of the functional determinants was obtained. In this representation the Casimir energy can be written in the form [27,28]

$$E(a) = \frac{1}{2\pi} \int_0^\infty d\xi \text{Tr} \ln(1 - \mathcal{T}^A \mathcal{G}_{\xi, AB}^{(0)} \mathcal{T}^B \mathcal{G}_{\xi, BA}^{(0)}) = \frac{1}{2\pi} \int_0^\infty d\xi \ln \det(1 - \mathcal{T}^A \mathcal{G}_{\xi, AB}^{(0)} \mathcal{T}^B \mathcal{G}_{\xi, BA}^{(0)}). \quad (25)$$

Here, $\mathcal{G}_{\xi, AB}^{(0)}$ is the operator for the free space Green function with the matrix elements $\langle \mathbf{r} | \mathcal{G}_{\xi, AB}^{(0)} | \mathbf{r}' \rangle$ where \mathbf{r} belongs to the body A and \mathbf{r}' to B . \mathcal{T}^A (\mathcal{T}^B) is the operator of the T -matrix

for a body A and B , respectively. The latter is widely used in light scattering theory, where it is the basic object for expressing the properties of the scatterers [29]. Using such a representation, in [28] the analytic results for the electromagnetic Casimir energy for an ideal metal cylinder above an ideal metal plane were obtained. Eventually, the result is expressed through the determinant of an infinite matrix with elements given in terms of the Bessel functions. The analytic asymptotic behavior of the exact Casimir energy at short separations was found in [30]. It results in the following expression for the Casimir force at $a \ll R$:

$$F^c(a, 0) = F_{\text{PFA}}^c(a) \left[1 - \frac{1}{5} \left(\frac{20}{\pi^2} - \frac{7}{12} \right) \frac{a}{R} \right]. \quad (26)$$

The PFA result (24) in this case matches with the first term on the right-hand side of (26).

Equation (26) is very important. It demonstrates that the relative error of the electromagnetic Casimir force between a cylinder and a plate calculated using the PFA is equal to $0.2886 a/R$. Thus, for typical experimental parameters of $R = 100 \mu\text{m}$ and $a = 100 \text{nm}$ this error is approximately equal to only 0.03%.

For a sphere above a plate made of ideal metals the exact analytic solution in the electromagnetic case has not yet been obtained. The scalar Casimir energy for a sphere above a plate was found in [30,31]. The scalar Casimir energies for both a sphere and a cylinder above a plate have also been computed numerically using the worldline algorithms [32,33], but it was noted that the Casimir energies for the Dirichlet scalar field should not be taken as an estimate for those in the electromagnetic case. For an ideal metal sphere above an ideal metal plane a correction of order a/R beyond the PFA was computed numerically in [34] for $a/R \geq 0.075$ and in [35] for $a/R \geq 0.15$. In both cases the extrapolation of the obtained results to smaller a/R leads to a coefficient near a/R approximately equal to 1.4.

In addition, the validity of the PFA for a sphere above a plate has been estimated experimentally [36] and the error introduced from the use of this approximation was shown to be less than a/R . This is in disagreement with the extrapolations made in [34,35]. To solve this contradiction, it is desirable to find the analytical form of the first correction beyond the PFA for a sphere above a plane, like in (26) for the cylinder-plane configuration.

In fact the representation (25) provides a far-reaching generalization of the Lifshitz formula. From conceptual point of view it can be applied not only to ideal metals, but to real materials as well. The problem, however, is to find the matrix elements of the T -matrix operator which would take proper account of both geometric shape and material properties of the test bodies used in the experimental situation.

4. The experimental error and reliability of experiments

The concept of the experimental error is often confused with the theoretical error and with the measure of agreement between experiment and theory. However, when we deal with an *independent measurement*, the experimental error has nothing to do with any theory of the measured quantity. The independent measurement of the Casimir force or its gradient does not use any theory of the Casimir effect. Thus, the experiments [4,5,37–42] are independent in this respect. In other experiments (in [43], for instance) the measurement data are fitted to some theoretical expression for the Casimir force. Such kind of measurements are not independent and we do not consider them below.

Some papers arrive to theoretical conclusions which are inconsistent with the measurement data. This is sometimes surrounded by the statement that the measurements might be not as precise as indicated by the authors. It is our opinion that such statements made without an indication of any specific cause are inappropriate. Both random, $\Delta^{\text{rand}} F^{\text{expt}}(a)$, and systematic, $\Delta^{\text{syst}} F^{\text{expt}}(a)$, experimental errors in the Casimir force measurements are found using the

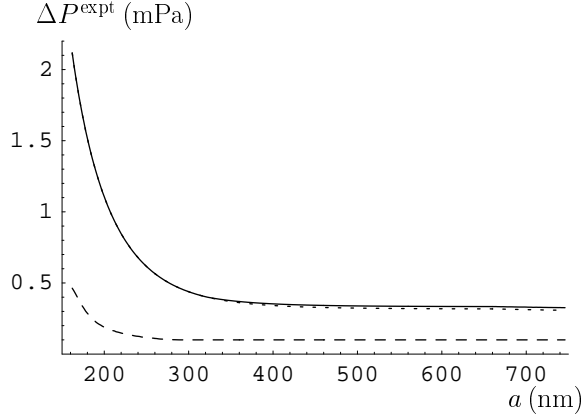


Figure 3. The total absolute experimental error of the Casimir pressure measurements [4,5] (the solid line), the random error (the long-dashed line), and the systematic error (the short-dashed line) are shown as functions of separation.

rigorous statistical procedures. They can be combined to find the total experimental error

$$\Delta^{\text{tot}} F^{\text{expt}}(a) = q_{\beta}(r) \left[\Delta^{\text{rand}} F^{\text{expt}}(a) + \Delta^{\text{syst}} F^{\text{expt}}(a) \right]. \quad (27)$$

Here, $q_{\beta}(r)$ determined at $\beta = 0.95$ (i.e., at 95% confidence level) varies between 0.71 and 0.81 depending of the value of the quantity $r = \Delta^{\text{syst}} F^{\text{expt}}(a) / s_{\bar{F}}(a)$, where $s_{\bar{F}}(a)$ is the variance of the mean measured quantity [44]. In fact there is no arbitrariness in the determination of the total experimental error which is the ultimate characteristic of the precision of the measurements. The most valuable experiments are marked by a negligible role of the random error. For such experiments

$$\Delta^{\text{tot}} F^{\text{expt}}(a) \approx \Delta^{\text{syst}} F^{\text{expt}}(a). \quad (28)$$

For today there is only one indirect measurement of the Casimir pressure between Au coated plates by means of micromechanical torsional oscillator satisfying this condition [4,5]. The total experimental error in this measurement at shortest separations is as small as 0.2% of the measured Casimir pressure. We stress once again that this error is unrelated to much larger errors inherent to theoretical computations on the basis of the Lifshitz theory or to the measure of agreement between experiment and theory. This is just the resulting error with which the experimental data are taken. As an example, the total absolute experimental error in the experiment on measuring the Casimir pressure by means of a micromechanical torsional oscillator [4,5] is shown in Fig. 3 as a function of separation (the solid line). The long-dashed and short-dashed lines show the random and systematic errors, respectively. As a result, the relative total experimental error $\delta^{\text{tot}} P^{\text{expt}}(a) = \Delta^{\text{tot}} P^{\text{expt}}(a) / |P^{\text{expt}}(a)|$ varies from 0.19% at $a = 162$ nm to 0.9% at $a = 400$ nm, and to 9.0% at $a = 746$ nm.

Sometimes the experimental precision can be questioned if there are some doubts in the calibration procedures used. For example, the electrostatic calibration is of prime importance in the independent measurements of the Casimir force. Specifically, it is usually carefully verified that the residual potential between the grounded test bodies does not depend on separation where the measurements of the electric force are performed. Recently it was claimed that the residual potential V_0 from the electrostatic calibration in the sphere-plate configuration is separation dependent [45]. The authors used an Au-coated sphere of 30.9 mm radius above an Au coated plate. On the basis of these measurements a reanalysis of the independence of V_0 on separation in the earlier measurements of the Casimir force by means of an atomic force microscope and a micromachined oscillator was invited. The results [45] are, however, not directly relevant to the earlier measurements. The point is that the radius of the sphere used in [45] is a factor of 300 larger than in the earlier precision measurements of the Casimir force. It

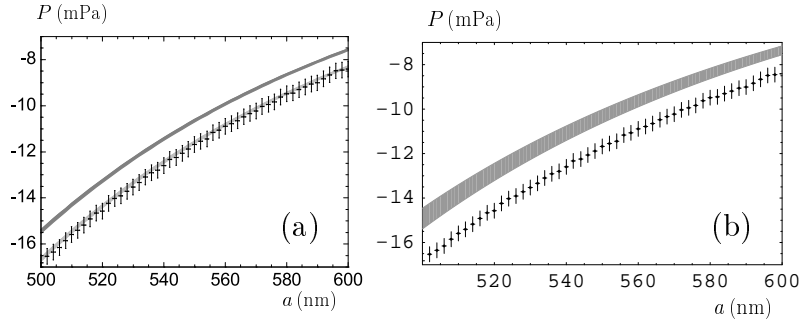


Figure 4. The crosses show the measured mean Casimir pressures together with the absolute errors in the separation and pressure as a function of the separation. (a) The theoretical Casimir pressures computed using the generalized plasma-like model and the optical data extrapolated by the Drude model are shown by the light-gray and dark-gray bands, respectively. (b) The theoretical Casimir pressures computed using different sets of optical data available in the literature versus separation are shown as the dark-gray band.

is well known that for large test bodies (i.e., large interaction areas) there are large variations of electric forces due to deviations of the mechanically polished and ground lens surface from perfect spherical shape [46].

5. Comparison between experiment and theory

Experiment is the supreme arbiter in physics. Because of this, the comparison between experiment and theory is a painful point for those theories that are found to be experimentally inconsistent. It happens that in such cases both the experimental data and the methods of comparison are questioned. The Casimir force is a strongly nonlinear function of the separation distance. As a consequence, such global characteristics of the agreement between experiment and theory as the root-mean-square deviation were found to be inadequate [47]. In the last few years two local methods on how to compare experiment with theory in the Casimir force measurements were elaborated and successfully applied. Within the first method [4,48,49], the experimental data are represented as crosses with arms determined by the total experimental errors in the measurement of separation and a related quantity (the force, the pressure or the frequency shift) determined at some chosen confidence level. In the same figure, one should plot the theoretical band whose width is equal to the total theoretical error determined at the same confidence as the experimental errors. The overlap (or its absence) of the experimental crosses and the theoretical band can be used to make a conclusion on the consistency or inconsistency between experiment and theory.

In Fig. 4 the first method of comparison between experiment and theory is illustrated on the measurement data by Decca et al. [4,5] discussed in Sec. 3. The light-gray band in Fig. 4(a) shows the theoretical results computed using the Lifshitz theory combined with the generalized plasma-like dielectric permittivity [50,51]

$$\varepsilon_{gp}(i\xi) = \varepsilon(i\xi) + \frac{\omega_p^2}{\xi^2}, \quad \varepsilon(i\xi) = 1 + \sum_{j=1}^K \frac{f_j}{\omega_j^2 + \xi^2 + \gamma_j \xi}. \quad (29)$$

Here, ω_p is the plasma frequency, $\omega_j \neq 0$ are the frequencies of the oscillators describing core electrons, f_j are the oscillator strengths and γ_j are the relaxation parameters. The dark-gray band in Fig. 4(a) is computed by the same Lifshitz theory using the tabulated optical data for Au [52] extrapolated to low frequencies by means of the Drude model [53–55]

$$\varepsilon_D(i\xi) = 1 + \frac{\omega_p^2}{\xi(\xi + \gamma)} = 1 + \frac{4\pi\sigma(i\xi)}{\xi}. \quad (30)$$

Here $\sigma(i\xi)$ is the conductivity. It is connected with the dc conductivity by the equation

$$\sigma(i\xi) = \frac{\sigma(0)}{1 + \frac{\xi}{\gamma}}. \quad (31)$$

Note that the plasma frequency and the dc conductivity are expressed as [56]

$$\omega_p^2 = \frac{4\pi e^2 n}{m}, \quad \sigma(0) = \mu |e| n, \quad (32)$$

where e and m are the charge and the mass of an electron, n is the charge carrier density and μ is their mobility. As is seen in Fig. 4(a), the experimental data shown as crosses (the experimental errors are determined at a 95% confidence level) are consistent with the theoretical approach using the generalized plasma-like permittivity. The Drude model approach is excluded at a 95% confidence level. In Fig. 4(b) the same experimental data are reproduced and compared with the Drude model approach using all sets of optical data available in the literature [57]. As is seen in Fig. 4(b), the use of optical data alternative to [52] makes the disagreement deeper between the experimental data and the Drude model approach. In Fig. 4(a,b) the comparison between experiment and theory is performed within the separation region from 500 to 600 nm. However, exactly the same conclusions follow over the entire measurement range in this experiment from 160 to 750 nm.

In the second method for the comparison of experiment and theory in the Casimir force measurements [40,48,58], the differences between the theoretical and mean experimental quantity, for instance, $P^{\text{theor}}(a) - \bar{P}^{\text{expt}}(a)$, are plotted as dots. In the same figure the borders of the confidence intervals $[-\Xi_P(a), \Xi_P(a)]$ for this difference at a chosen confidence level (usually 95%) are plotted as the function of separation. If no less than 95% of the dots representing the above differences belong to the confidence interval the theoretical approach is consistent with the data. Alternatively, if almost all the dots are outside the confidence interval, the theoretical approach is excluded by the data at a 95% confidence level. In Fig. 5 we illustrate the second method for the comparison of experiment with theory using the experimental data of the same measurements [4,5]. In Fig. 5(a) the theoretical approach using the generalized plasma-like permittivity (29) is compared with the data. It is seen that all dots are inside the

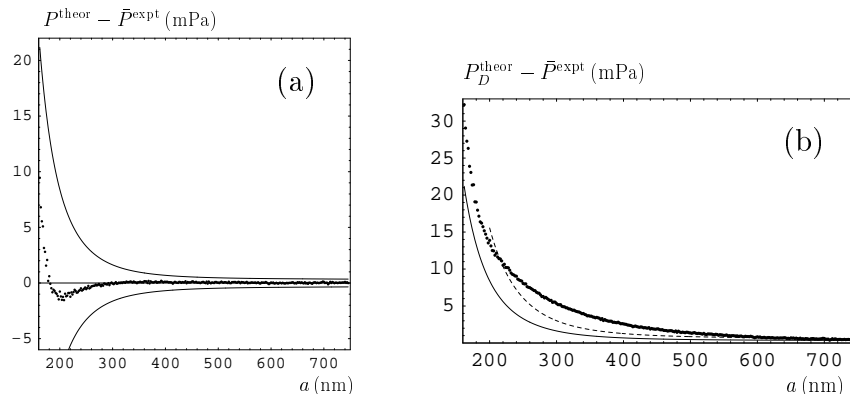


Figure 5. The differences of the theoretical and the mean experimental Casimir pressures between the two Au plates versus separation are shown as dots. The theoretical results are calculated using the Lifshitz theory at room temperature using (a) the generalized plasma-like model and (b) the Drude model approach. The solid lines indicate the boundaries of the 95% confidence intervals. The dashed line indicates the boundary of the 99.9% confidence intervals.

error bars. Thus, this approach is consistent with the data. In Fig. 5(b) the same data are compared with the theoretical approach using the tabulated optical data extrapolated by the Drude model. The solid and dashed line represent the borders of 95% and 99.9% confidence intervals, respectively. As is seen in Fig. 5(b), the Drude model approach is experimentally excluded at a 95% confidence level within the entire measurement range from 160 to 750 nm. Within a more narrow measurement range from 210 to 620 nm the Drude model approach is excluded at a 99.9% confidence level.

If the theoretical approach is experimentally consistent [see Fig. 5(a)] the quantity $\Xi_P/|\bar{P}^{\text{expt}}|$, determined at a 95% confidence level, can be used as the quantitative measure of agreement between experiment and theory. Thus, at $a = 162$ nm this measure is equal to 1.9%. It decreases to 1.4% at $a = 300$ nm and then gradually increases up to 9.7% at $a = 745$ nm. It is evident that at the shortest separation the agreement between experiment and theory is almost an order of magnitude worse than the total experimental error equal to only 0.19%. This is explained by large theoretical errors which dominate in the determination of Ξ_P at the shortest separations.

The above explanations aim to make absolutely clear that the calculation of errors and the comparison between experiment and theory is not an arbitrary, but a rigorously determined procedure. Recently, the measurement data of the experiment [4,5] was independently reanalyzed in [59] with the conclusion: “The data rule out the Drude approach. . . , while they are consistent with the plasma-model approach. . .”

6. Attempt to account for screening effects

Recently, the above discussed problems of the Drude model approach in application to real metals, and related problems arising for dielectric and semiconductor materials [60–64], motivated an attempt to modify the reflection coefficients in the Lifshitz formula by including the screening effects and diffusion currents [65,66]. The modified reflection coefficients for the transverse magnetic and transverse electric modes were obtained through use of Boltzmann transport equation which takes into account not only the standard drift current \mathbf{j} , but also the diffusion current $eD\nabla n$, where D is the diffusion coefficient and ∇n is the gradient of the charge carrier density [66]. The transverse magnetic coefficient takes the form

$$\tilde{r}_{\text{TM}}(i\xi, k_{\perp}) = \frac{\tilde{\varepsilon}(i\xi)q - k - \frac{k_{\perp}^2}{\eta(i\xi)} \frac{\tilde{\varepsilon}(i\xi) - \varepsilon(i\xi)}{\varepsilon(i\xi)}}{\tilde{\varepsilon}(i\xi)q + k + \frac{k_{\perp}^2}{\eta(i\xi)} \frac{\tilde{\varepsilon}(i\xi) - \varepsilon(i\xi)}{\varepsilon(i\xi)}}, \quad (33)$$

where k_{\perp} is the projection of the wave vector in the plane of the plates, $\omega = i\xi$ is the imaginary frequency and the following notations are introduced

$$q^2 = k_{\perp}^2 + \frac{\xi^2}{c^2}, \quad k^2 = k_{\perp}^2 + \tilde{\varepsilon}(i\xi) \frac{\xi^2}{c^2}, \quad \tilde{\varepsilon}(i\xi) = \varepsilon(i\xi) + \frac{\omega_p^2}{\xi(\xi + \gamma)},$$

$$\eta(i\xi) = \left[k_{\perp}^2 + \kappa^2 \frac{\varepsilon(0)}{\varepsilon(i\xi)} \frac{\tilde{\varepsilon}(i\xi)}{\tilde{\varepsilon}(i\xi) - \varepsilon(i\xi)} \right]^{1/2}. \quad (34)$$

In this equation, $1/\kappa$ is the screening length and the dielectric permittivity of core electrons $\varepsilon(i\xi)$ is defined in (29). The transverse electric coefficient is given by the standard expression

$$\tilde{r}_{\text{TE}}(i\xi, k_{\perp}) = \frac{q - k}{q + k}, \quad (35)$$

as is used in the Drude model approach.

The paper [66] claims the application of the above approach to intrinsic semiconductors only. It uses a specific Debye-Hückel expression for the screening length

$$\frac{1}{\kappa} = \frac{1}{\kappa_{\text{DH}}} = R_{\text{DH}} = \sqrt{\frac{\varepsilon(0)k_B T}{4\pi e^2 n}}. \quad (36)$$

This expression is applicable to particles obeying the Maxwell-Boltzmann statistics. It is obtained from the general representation for the screening length [67]

$$\frac{1}{\kappa} = R = \sqrt{\frac{\varepsilon(0)D}{4\pi\sigma(0)}} \quad (37)$$

if one uses the expression (32) for the dc conductivity and Einstein's relation [56,67]

$$\frac{D}{\mu} = \frac{k_B T}{|e|} \quad (38)$$

valid in the case of Maxwell-Boltzmann statistics. In the limiting case $\xi \rightarrow 0$ the reflection coefficient (33) coincides with that obtained in [65].

However, the application region of the reflection coefficients (33), (34) with the Debye-Hückel screening length (36) cannot be restricted to only intrinsic semiconductors. These coefficients should be applicable to all materials where the density of charge carriers is not too large so that they are described by Maxwell-Boltzmann statistics. This means that in the framework of the proposed approach it is legal to apply (33)–(36) to doped semiconductors with dopant concentration below critical and to solids with ionic conductivity etc.

Here, we consider the application of this approach to metallic plates. Metals and semiconductors of metallic type are characterized by rather high concentration of charge carriers which obey the quantum Fermi-Dirac statistics. The general transport equation, however, is equally applicable to classical and quantum systems. The only difference one should take into account is the type of statistics. Substituting Einstein's relation, valid in the case of Fermi-Dirac statistics [56,67]

$$\frac{D}{\mu} = \frac{2E_F}{3|e|}, \quad (39)$$

where $E_F = \hbar\omega_p$ is the Fermi energy, into (37), one arrives to the following expression for the Thomas-Fermi screening length [67]

$$\frac{1}{\kappa} = \frac{1}{\kappa_{\text{TF}}} = R_{\text{TF}} = \sqrt{\frac{\varepsilon(0)E_F}{6\pi e^2 n}}. \quad (40)$$

With this definition of the parameter κ , it is legal to apply equations (33)–(35) to metals.

Now we consider two thick metallic plates separated by a distance a at temperature T in thermal equilibrium. Under these conditions the Casimir free energy per unit area of the plates is given by the Lifshitz formula [68]. Let us assume that the reflection coefficients (33)–(35), (40) can be substituted into this formula. Then in terms of dimensionless variables $y = 2aq$, $\zeta = \xi/\omega_c \equiv 2a\xi/c$ one obtains

$$\tilde{\mathcal{F}}(a, T) = \frac{k_B T}{8\pi a^2} \sum_{l=0}^{\infty}{}' \int_{\zeta_l}^{\infty} y dy \left\{ \ln \left[1 - \tilde{r}_{\text{TM}}^2(i\zeta_l, y) e^{-y} \right] + \ln \left[1 - \tilde{r}_{\text{TE}}^2(i\zeta_l, y) e^{-y} \right] \right\}, \quad (41)$$

where $\zeta_l = 4\pi a k_B T l / (\hbar c)$ are the dimensionless Matsubara frequencies and a prime near the summation sign adds a multiple 1/2 to the term with $l = 0$. In terms of the dimensionless variables the reflection coefficient (33) takes the form

$$\tilde{r}_{\text{TM}}(i\zeta, y) = \frac{\tilde{\varepsilon}y - [y^2 + (\tilde{\varepsilon} - 1)\zeta^2]^{1/2} - \frac{(y^2 - \zeta^2)(\tilde{\varepsilon} - \varepsilon)}{\tilde{\eta}\varepsilon}}{\tilde{\varepsilon}y + [y^2 + (\tilde{\varepsilon} - 1)\zeta^2]^{1/2} + \frac{(y^2 - \zeta^2)(\tilde{\varepsilon} - \varepsilon)}{\tilde{\eta}\varepsilon}}, \quad (42)$$

where

$$\tilde{\eta} = 2a\eta = \left[y^2 - \zeta^2 + \kappa_a^2 \frac{\varepsilon(0)\tilde{\varepsilon}}{\varepsilon(\tilde{\varepsilon} - \varepsilon)} \right]^{1/2}, \quad \kappa_a \equiv 2a\kappa_{\text{TF}}. \quad (43)$$

Note that all dielectric permittivities here are functions of $i\omega_c\zeta$. Below we do not use the explicit expression for the reflection coefficient $\tilde{r}_{\text{TE}}(i\zeta, y)$ because it coincides with the standard one, as defined in the Drude model approach, and considered in detail in [69].

Let us determine the behavior of the Casimir free energy (41) at low temperature. For all metals the screening length (40) is very small. As a result, at any reasonable separation distance between the plates, the dimensionless parameter κ_a defined in (43) is very large and the inverse quantity can be used as a small parameter

$$2a\kappa_{\text{TF}} = \kappa_a \gg 1, \quad \beta_a \equiv \frac{1}{\kappa_a} \ll 1. \quad (44)$$

Expanding the reflection coefficient (42) up to the first power of the parameter β_a one obtains

$$\begin{aligned} \tilde{r}_{\text{TM}}(i\zeta, y) &= r_{\text{TM}}(i\zeta, y) - 2\beta_a Z + O(\beta_a^2), \\ Z &\equiv \sqrt{\frac{\tilde{\varepsilon}(\tilde{\varepsilon} - \varepsilon)^3}{\varepsilon(0)\varepsilon} \frac{y(y^2 - \zeta^2)}{[\tilde{\varepsilon}y + \sqrt{y^2 + (\tilde{\varepsilon} - 1)\zeta^2}]^2}}, \end{aligned} \quad (45)$$

where $r_{\text{TM}}(i\zeta, y)$ is the standard TM reflection coefficient calculated with the dielectric permittivity $\tilde{\varepsilon}(i\omega_c\zeta)$ [it is given by (42) with the third term in both numerator and denominator omitted]. From (45) one arrives at

$$\ln \left[1 - \tilde{r}_{\text{TM}}^2(i\zeta, y) e^{-y} \right] = \ln \left[1 - r_{\text{TM}}^2(i\zeta, y) e^{-y} \right] + 4\beta_a \frac{r_{\text{TM}}(i\zeta, y) Z}{e^y - r_{\text{TM}}^2(i\zeta, y)} + O(\beta_a^2). \quad (46)$$

Now we substitute (46) and the respective known expression for the TE contribution [69] into (41). Calculating the sum with the help of the Abel-Plana formula, we obtain in perfect analogy to [69]

$$\tilde{\mathcal{F}}(a, T) = \mathcal{F}_{gp}(a, T) - \frac{k_B T}{16\pi a^2} \int_0^\infty y dy \ln \left[1 - r_{\text{TE},gp}^2(0, y) e^{-y} \right] + \mathcal{F}^{(\gamma)}(a, T) + \beta_a \mathcal{F}^{(\beta)}(a, T), \quad (47)$$

where $\mathcal{F}^{(\gamma)}(a, T)$ is determined by equation (17) in [69]. It goes to zero together with its derivative with respect to temperature when $T \rightarrow 0$. The quantity $\mathcal{F}^{(\beta)}(a, T)$ originates from the second contribution on the right-hand side of (45). It is easily seen that $\mathcal{F}^{(\beta)}(a, T) = E^{(\beta)}(a) + O(T^3/T_{\text{eff}}^3)$ at low T . The Casimir free energy $\mathcal{F}_{gp}(a, T)$ is defined by substituting the dielectric permittivity (29) of the generalized plasma-like model into the Lifshitz formula. It was found in [50,51] and the respective thermal correction was shown to be of order $(T/T_{\text{eff}})^3$ when $T \rightarrow 0$. The TE reflection coefficient at zero frequency entering (47) is given by

$$r_{\text{TE},gp}(0, y) = \frac{cy - \sqrt{4a^2\omega_p^2 + c^2y^2}}{cy + \sqrt{4a^2\omega_p^2 + c^2y^2}}. \quad (48)$$

As a result, calculating the Casimir entropy

$$\tilde{S}(a, T) = -\frac{\partial \tilde{\mathcal{F}}(a, T)}{\partial T} \quad (49)$$

with the use of (47) and considering the limiting case of zero temperature, one arrives at

$$\tilde{S}(a, 0) = \frac{k_B}{16\pi a^2} \int_0^\infty y dy \ln \left[1 - \left(\frac{cy - \sqrt{4a^2\omega_p^2 + c^2y^2}}{cy + \sqrt{4a^2\omega_p^2 + c^2y^2}} \right)^2 e^{-y} \right] < 0 \quad (50)$$

in violation of the Nernst heat theorem. This result is obtained for metals with perfect crystal lattices. In the presence of impurities the Casimir entropy abruptly jumps to zero at $T < 10^{-3}$ K [70].

Thus, the modified reflection coefficients taking the screening effects into account lead to a violation of the Nernst heat theorem for metals with perfect crystal lattices in the same way as the standard Drude model approach. Because of this, the theoretical approach using such reflection coefficients is thermodynamically inconsistent.

Now we briefly compare the theoretical predictions, following from the use of reflection coefficients \tilde{r}_{TM} and \tilde{r}_{TE} , with the measurement data of the most precise experiment by means of micromachined torsional oscillator [4,5]. This experiment was already discussed in Sec. 5. In Fig. 6(a) the experimental data for the Casimir pressure between two Au plates are shown as crosses with the absolute errors determined at a 95% confidence level. The solid line presents the computational results for $P(a, T) = -\partial\mathcal{F}(a, T)/\partial a$ using the Lifshitz formula and the generalized plasma-like dielectric permittivity (29). The parameters of oscillators for Au were determined in [5] with high precision. The dashed line was computed using the Lifshitz formula for $P^{\text{mod}}(a, T) = -\partial\tilde{\mathcal{F}}(a, T)/\partial a$ with the reflection coefficients $\tilde{r}_{\text{TM,TE}}$ taking the screening effects into account. As is seen in Fig. 6(a), the theoretical approach taking into account the Thomas-Fermi screening length is experimentally excluded at a 95% confidence level over the separation region from 500 to 600 nm. The same conclusion follows within the entire measurement range from 160 to 750 nm.

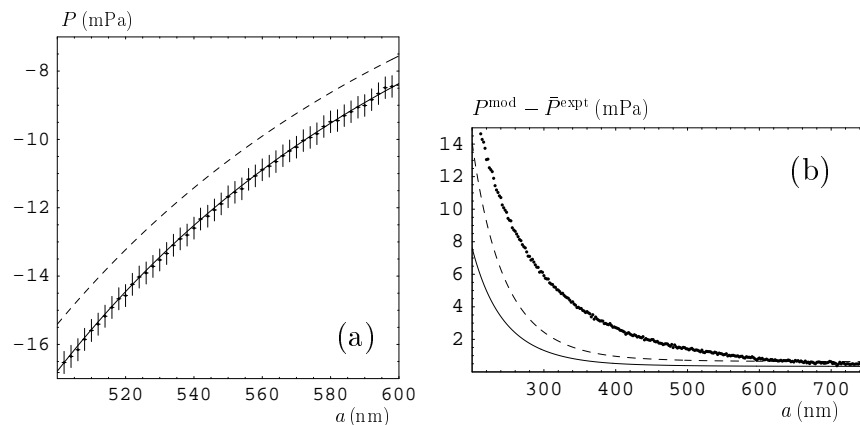


Figure 6. (a) The crosses show the measured mean Casimir pressures together with the absolute errors as a function of the separation. The theoretical Casimir pressures computed using the generalized plasma-like model and the approach including the screening effects are shown as solid and dashed lines, respectively. (b) Differences of the theoretical Casimir pressures computed with inclusion of the screening effects and the mean experimental Casimir pressures versus separation are shown as dots. The 95% and 99.9% confidence intervals are shown as the solid and dashed lines, respectively.

Fig. 6(a) illustrates the first method for the comparison between experiment and theory in Casimir force measurements discussed in Sec. 5. In Fig. 6(b) the second method for the comparison of experiment and theory is illustrated. Here, the differences between the theoretical Casimir pressures computed with inclusion of the screening effects and the mean experimental pressures are shown as dots. The solid line indicates the borders of 95% confidence intervals. Dots are outside the confidence interval $[-\Xi_P(a), \Xi_P(a)]$ over the entire measurement range from 160 to 750 nm. In the same figure, the dashed line shows the borders of 99.9% confidence intervals. As is seen in Fig. 6(b), dots are outside of this confidence interval within the separation region from 160 to 640 nm. Thus, within this region of separations the theoretical approach taking the screening effects into account [66] is experimentally excluded at a 99.9% confidence level.

The physical reasons why the inclusion of the screening effects into the Lifshitz theory is thermodynamically and experimentally inconsistent can be understood as follows. The Lifshitz theory is formulated for systems in thermal equilibrium. As was indicated in [71], the drift current of conduction electrons leads to heating of the crystal lattice. In this case, if the constant temperature is preserved, there must be a unidirectional flux of heat from the Casimir plates to the heat reservoir. The existence of such an interaction between a system and a heat reservoir is strictly prohibited in a state of thermal equilibrium [72] and is in contradiction with its definition [73]. According to this definition, in thermal equilibrium all irreversible processes connected with the dissipation of energy are terminated. Specifically, in thermal equilibrium any nonzero gradients of charge carrier density and any diffusion are impossible. Thus, the inclusion of the screening effects and diffusion currents into the Lifshitz theory is in violation of its applicability conditions.

7. Conclusions and discussion

In the above, we have discussed several problems at the interface between field-theoretical description of the Casimir effect and experiments on measuring the Casimir force. The consideration of the Casimir energies and forces in ideal metal rectangular boxes leads to the conclusion that even when using ideal models it is important to take into account some general physical requirements. Thus, it is not productive to use the free energy which leads to the Casimir forces of quantum nature which increase with increasing size of the box. It also seems thermodynamically inconsistent to claim that the Casimir force acting on a piston is a well defined quantity, whereas the forces acting on all other faces of the box are excluded from consideration. The reason is that if the free energy is defined correctly (see Sec. 2), there is a uniquely defined pressure on all faces of the box equal to the negative derivative of the free energy with respect to the box volume calculated at constant temperature.

An important tool for the comparison of experiment with theory is the proximity force approximation. In Sec. 3 we have discussed some inexact formulations which can be found in theoretical publications on this subject. We have also discussed recent achievements in quantum-field-theoretical approach to the calculation of the Casimir energies in terms of functional determinants and scattering matrices. This scientific direction has already obtained the first analytical results beyond the PFA. It is of great promise for many experimentally relevant applications of the theory.

In Secs. 4 and 5 we tried to add clarity to the widely discussed problems of the precision of experiments on the Casimir effect and the agreement between experiment and theory. It was stressed that the precision of some independent measurements can be much higher than of respective theoretical computations using the values of parameters which may not be known precisely enough. In such cases the agreement of experiment with theory can also be not as good as the precision of the measurements.

Finally, in Sec. 6 we have analyzed a recent theoretical approach to the thermal Casimir

force taking into account the screening effects and diffusion currents. Using quantum Fermi-Dirac statistics and respective Thomas-Fermi screening length, we have applied this approach to calculate the Casimir free energy between two metallic plates. It was shown that the obtained free energy results in a violation of the Nernst heat theorem for metals with perfect crystal lattices. Thus, the approach under consideration is inconsistent with thermodynamics. The calculational results for the Casimir pressure in the configuration of two Au plates were compared with the results of the most precise experiment performed using a micromachined oscillator. It was shown that the theoretical predictions following from the inclusion of the screening effects are rejected by the experimental data at a 99.9% confidence level. The reason for the failure of this approach is the inclusion of irreversible diffusion processes violating thermal equilibrium which is the basic applicability condition of the Lifshitz theory.

Phenomenologically, the Lifshitz theory combined with the generalized plasma-like dielectric permittivity provides a description of dispersion forces between metallic test bodies which is in agreement with thermodynamics and consistent with all available experimental information. For now there is no other theoretical approach to the thermal Casimir force between metals which would satisfy the requirements of thermodynamics and be simultaneously consistent with all measurement data.

Acknowledgments

This work was supported by Deutsche Forschungsgemeinschaft, Grant No 436 RUS 113/789/0–4. The author is grateful to the Center of Theoretical Studies and Institute of Theoretical Physics, Leipzig University where this work was performed for kind hospitality.

- [1] Casimir H B G 1948 *Proc. K. Ned. Akad. Wet.* **51** 793
- [2] Sparnaay M J 1958 *Physica* **24** 751
- [3] van Blokland P H G M and Overbeek J T G 1978 *J. Chem. Soc. Faraday Trans.* **74** 2637
- [4] Decca R S, López D, Fischbach E, Klimchitskaya G L, Krause D E and Mostepanenko V M 2007 *Phys. Rev. D* **75** 077101
- [5] Decca R S, López D, Fischbach E, Klimchitskaya G L, Krause D E and Mostepanenko V M 2007 *Eur. Phys. J. C* **51** 963
- [6] Lukosz W 1971 *Physica* **56** 109
- [7] Mamayev S G and Trunov N N 1979 *Teor. Matem. Fiz.* **38** 345 (*Theor. Math. Phys.* **38** 228)
- [8] Mamayev S G and Trunov N N 1979 *Izv. Vuzov, Fizika* N9 51 (*Rus. Phys. J.* **22** 966)
- [9] Ambjørn J and Wolfram S 1983 *Ann. Phys., N.Y.* **147** 1
- [10] Bordag M, Mohideen U and Mostepanenko V M 2001 *Phys. Rep.* **353** 1
- [11] Cavalcanti R M 2004 *Phys. Rev. D* **69** 065015
- [12] Hertzberg M P, Jaffe R L, Kardar M and Scardicchio A 2005 *Phys. Rev. Lett.* **95** 250402
- [13] Hertzberg M P, Jaffe R L, Kardar M and Scardicchio A 2007 *Phys. Rev. D* **76** 045016
- [14] Ederly A 2007 *Phys. Rev. D* **75** 105012
- [15] Zhai X-H and Li X-Z 2007 *Phys. Rev. D* **76** 047704
- [16] Charlton T M 1973 *Energy Principles in Theory of Structures* (Oxford: Oxford University Press)
- [17] Langhaar H L 1989 *Energy Methods in Applied Mechanics* (Brooklyn: Krieger Press)
- [18] Kubo R 1968 *Thermodynamics* (Amsterdam: North-Holland Publishing Company)
- [19] Santos F C and Tort A 2000 *Phys. Lett. B* **482** 323
- [20] Jáuregui R, Villarreal C and Hacyan S 2006 *Ann. Phys., NY* **321** 2156
- [21] Lim S C and Teo L P 2007 *J. Phys. A: Math. Theor.* **40** 11645
- [22] Dowker J S and Kennedy G 1978 *J. Phys. A: Math. Gen.* **11** 895
- [23] Geyer B, Klimchitskaya G L and Mostepanenko V M 2008 *Eur. Phys. J. C* **57** 823
- [24] Brown L S and Maclay G J 1969 *Phys. Rev.* **184** 1272
- [25] Lim S C and Teo L P 2008 Casimir piston at zero and finite temperature. *Preprint* arXiv:0808.0047
- [26] Blocki J, Randrup J., Swiatecki W J and Tsang C F 1977 *Ann. Phys., NY* **105** 427.
- [27] Kenneth O and Klich I 2006, *Phys. Rev. Lett.* **97** 0160401
- [28] Emig T, Jaffe R L, Kardar M and Scardicchio A 2006 *Phys. Rev. Lett.* **96** 080403
- [29] Bohren C F and Huffman D R 1998 *Absorption and Scattering of Light by Small Particles* (New York: Wiley)
- [30] Bordag M 2006 *Phys. Rev. D* **73** 125018

- [31] Bulgac A, Magierski P and Wirzba A 2006 *Phys. Rev. D* **73** 025007
- [32] Gies H and Klingmüller K 2006 *Phys. Rev. Lett.* **96** 220401
- [33] Gies H and Klingmüller K 2006 *Phys. Rev. D* **74** 045002
- [34] Emig T 2008 *J. Stat. Mech.* P04007
- [35] Maia Neto P A, Lambrecht A and Reynaud S 2008 *Phys. Rev. A* **78** 012115
- [36] Krause D E, Decca R S, López D and Fischbach E 2007 *Phys. Rev. Lett.* **98** 050403
- [37] Harris B W, Chen F and Mohideen U 2000 *Phys. Rev. A* **62** 052109
- [38] Chen F, Klimchitskaya G L, Mohideen U and Mostepanenko V M 2004 *Phys. Rev. A* **69** 022117
- [39] Decca R S, Fischbach E, Klimchitskaya G L, Krause D E, López D and Mostepanenko V M 2003 *Phys. Rev. D* **68** 116003
- [40] Decca R S, López D, Fischbach E, Klimchitskaya G L, Krause D E and Mostepanenko V M 2005 *Ann. Phys. NY* **318** 37
- [41] Jourdan G, Lambrecht A, Comin F and Chevrier J 2009 *Europhys. Lett.* **85** 31001
- [42] Chan H B, Bao Y, Zou J, Cirelli R A, Clemens F, Mansfield W M and Pai C S 2008 *Phys. Rev. Lett.* **101** 030401
- [43] Bressi G, Carugno G, Onofrio R. and Ruoso G 2002 *Phys. Rev. Lett.* **88** 041804
- [44] Rabinovich S G 2000 *Measurement Errors and Uncertainties. Theory and Practice* (New York: Springer-Verlag)
- [45] Kim W J, Brown-Hayes M, Dalvit D A R, Brownell J H and Onofrio R 2008 *Phys. Rev. A* **78** 020101(R)
- [46] Decca R S, Fischbach E, Klimchitskaya G L, Krause D E, López D, Mohideen U and Mostepanenko V M 2009 *Phys. Rev. A* **79** 026101
- [47] Ederth T 2000 *Phys. Rev. A* **62** 062104
- [48] Chen F, Mohideen U, Klimchitskaya G L and Mostepanenko V M 2006 *Phys. Rev. A* **74** 022103
- [49] Obrecht J M, Wild R J, Antezza M, Pitaevskii L P, Stringari S and Cornell E A 2007 *Phys. Rev. Lett.* **98** 063201
- [50] Geyer B, Klimchitskaya G L and Mostepanenko V M 2007 *J. Phys. A: Math. Theor.* **40** 13485
- [51] Mostepanenko V M and Geyer B 2008 *J. Phys. A: Mat. Theor.* **41** 164014
- [52] Palik E D (ed) 1985 *Handbook of Optical Constants of Solids* (New York: Academic)
- [53] Boström M and Sernelius B E 2000 *Phys. Rev. Lett.* **84** 4757
- [54] Brevik I, Aarseth J B, Høye J S and Milton K A 2005 *Phys. Rev. E* **71** 056101
- [55] Milton K A 2004 *J. Phys. A: Math. Gen.* **37** R209
- [56] Ashcroft N W and Mermin N D 1976 *Solid State Physics* (Philadelphia: Saunders College)
- [57] Pirozhenko I, Lambrecht A and Svetovoy V B 2006 *New J. Phys.* **8** 238
- [58] Chen F, Klimchitskaya G L, Mostepanenko V M and Mohideen U 2006 *Phys. Rev. Lett.* **97** 170402
- [59] Bimonte G 2007 The thermal Casimir effect for rough metallic plates *Preprint* arXiv:0711.0278
- [60] Geyer B, Klimchitskaya G L and Mostepanenko V M 2005 *Phys. Rev. D* **72** 085009
- [61] Geyer B, Klimchitskaya G L and Mostepanenko V M 2006 *Int. J. Mod. Phys. A* **21** 5007
- [62] Geyer B, Klimchitskaya G L and Mostepanenko V M 2008 *Ann. Phys. NY* **323** 291
- [63] Klimchitskaya G L and Geyer B 2008 *J. Phys. A.: Mat. Theor.* **41** 164032
- [64] Ellingsen S A, Brevik I, Høye J S and Milton K A 2008 *Phys. Rev. E* **78** 021117
- [65] Pitaevskii L P 2008 *Phys. Rev. Lett.* **101** 163202
- [66] Dalvit D A R and Lamoreaux S K 2008 *Phys. Rev. Lett.* **101** 163203
- [67] Chazalviel J-N 1999 *Coulomb Screening of Mobile Charges: Applications to Material Science, Chemistry and Biology* (Boston: Birkhauser)
- [68] Lifshitz E M 1956 *Zh. Eksp. Teor. Fiz.* **29** 94 (*Sov. Phys. JETP* **2** 73)
- [69] Bezerra V B, Klimchitskaya G L, Mostepanenko V M and Romero C 2004 *Phys. Rev. A* **69** 022119
- [70] Høye J S, Brevik I, Ellingsen S A and Aarseth J B 2007 *Phys. Rev. E* **75** 051127
- [71] Geyer B, Klimchitskaya G L and Mostepanenko V M 2003 *Phys. Rev. A* **67** 062102
- [72] Bryksin V V and Petrov M P 2008 *Fiz. Tverdogo Tela* **50** 222 (*Phys. Solid State* **50** 229)
- [73] Kondepudi D and Prigogine I 1998 *Modern Thermodynamics* (New York: Wiley)